

Rates and Mechanism of Proton Transfer from Transient Carbon Acids. The Acidities of Methylbenzene Cations

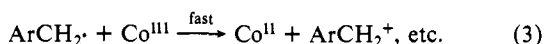
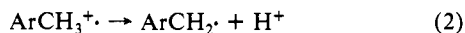
C. J. Schlesener, C. Amatore, and J. K. Kochi*†

Contribution from the Department of Chemistry, Indiana University, Bloomington, Indiana 47405. Received January 9, 1984

Abstract: The fast rates of proton transfer from various methylbenzene cation radicals to a series of substituted pyridine bases are successfully measured in acetonitrile solutions. The technique utilizes the production of the cation radical as a transient intermediate during the electron-transfer oxidation of the methylbenzene with an iron(III) oxidant. Complete analysis of the complex kinetics affords reliable values of the deprotonation rate constants k_2 which span a range from 3×10^2 to more than $2 \times 10^7 \text{ M}^{-1} \text{ s}^{-1}$. The relative acidities of the cation radicals of hexamethylbenzene, pentamethylbenzene, durene, and prehnitene can be obtained from the Brønsted correlation of the deprotonation rate constants with the pyridine base strengths and the standard oxidation potentials of the methylarenes. An estimate of the acidity constant for the hexamethylbenzene cation radical is based on several empirical extrapolations to that of the toluene cation radical previously evaluated by Nicholas and Arnold on thermochemical grounds. The kinetic acidities of the various methylarene cation radicals are also examined in the context of the Marcus equation, as applied to proton transfer. The mechanism of proton transfer from these labile carbon acids is discussed with regard to the electronic effects relevant to the methylarene oxidation potential and the pyridine base strength, the kinetic isotope effects with deuterated methyl groups, the salt effects in acetonitrile, and the steric effects of ortho substituents on pyridine.

Aromatic hydrocarbons are subject to the oxidative degradation of the alkyl side chains, as in the industrially important cobalt-catalyzed conversion of *p*-xylene to terephthalic acid.^{1,2} The results of numerous studies of the reaction of cobalt (III) complexes with various methylbenzenes (ArCH_3) are compatible with the initial steps³⁻⁸ shown in Scheme I. According to the qualitative mechanism outlined in Scheme I, the degradation of the alkyl side chain commences by prior electron transfer in eq 1, followed by the loss of an α -proton from the methylbenzene radical cation in eq 2, and subsequent rapid oxidation of the benzylic radical in eq 3.

Scheme I



As part of our interest in organic oxidations,⁹ we have undertaken a comprehensive mechanistic study of the structural features of different methylbenzenes in relation to the rate of each step in the oxidation process. Thus we have recently demonstrated how a related series of coordinatively saturated tris(phenanthroline)iron(III) complexes FeL_3^{3+} can be exploited as oxidants for the study of the initial electron transfer from aromatic hydrocarbons (compare eq 1). These iron(III) complexes are sufficiently well-behaved in solution to allow for meaningful kinetic studies (i.e., they are substitution inert), and their reduction potentials E°_{Fe} can be varied systematically by nuclear substitution in the phenanthroline ligand.¹⁰⁻¹² Similarly, an appropriate choice of methylbenzenes enables their donor properties, given by the reversible potentials E°_{Ar} , to be varied systematically.¹³ In this manner, various methylbenzenes have been oxidatively converted by these iron(III) complexes in the presence of bases (B) according to the overall stoichiometry:¹⁴



which is equivalent to that in Scheme I. The systematic study of the kinetics, products, and structural effects of methylbenzenes and FeL_3^{3+} has established the sequence of fundamental steps, labeled with their appropriate rate constants, shown in Scheme II.

Scheme II



The methylbenzene cation radical $\text{ArCH}_3^{\cdot+}$ formed in eq 5 can be observed as the prime intermediate by kinetic ESR spectroscopy. Its formation by electron transfer proceeds via an outer-sphere mechanism since the experimental free energy relationship established for the rate constant ($\log k_1$) with the measured driving force $\mathcal{F}(E^\circ_{\text{Ar}} - E^\circ_{\text{Fe}})$ is in quantitative accord with the predictions of the Marcus rate theory.¹⁵ We have also shown in a separate study¹⁶ that the oxidation of benzyl radicals by FeL_3^{3+} as in eq 7, is an extremely facile process ($k_3 > 10^6 \text{ M}^{-1} \text{ s}^{-1}$) and proceeds

(1) Hucknall, D. J. "Selective Oxidation of Hydrocarbons"; Academic Press: New York, 1974.

(2) Landau, R.; Saffer, A. *Chem. Eng. Prog.* **1968**, *64*, 20.

(3) For a review, see: Sheldon, R. A.; Kochi, J. K. In "Metal Catalyzed Oxidation of Organic Compounds"; Academic Press: New York, 1981.

(4) Beletskaya, I. P.; Makhon'kov, D. I. *Russ. Chem. Rev. (Engl. Transl.)* **1981**, *50*, 1007.

(5) Ebersson, L. *J. Am. Chem. Soc.* **1983**, *105*, 3192.

(6) Andrusis, P. J.; Dewar, M. J. S.; Deitz, R.; Hunt, R. L. *J. Am. Chem. Soc.* **1966**, *88*, 5473.

(7) Jones, G. H. *J. Chem. Res.* **1981**, 228; **1982**, 207.

(8) For studies of the related anodic oxidations, see: (a) Nyberg, K. In "Encyclopedia of Electrochemistry of the Elements"; Bard, A. J., Lund, H., Eds. Marcel Dekker: New York, 1978; Vol. XI, Chapter IX-1, pp 43-70. (b) Ebersson, L.; Nyberg, K. *Acc. Chem. Res.* **1973**, *6*, 106 and references therein.

(c) Baumberger, R. S.; Parker, V. D. *Acta Chem. Scand., Ser. B* **1980**, *B34*, 537. (d) Bewick, A.; Edwards, G. J.; Mellor, J. M.; Pons, B. S. *J. Chem. Soc., Perkin Trans. 2* **1977**, 1952.

(9) Kochi, J. K.; Tang, R. T.; Bernath, T. *J. Am. Chem. Soc.* **1973**, *95*, 7114.

(10) Schilt, A. A. "Analytical Applications of 1,10-Phenanthroline and Related Compounds"; Pergamon: Oxford, 1969.

(11) See, e.g.: (a) Dulz, G.; Sutin, N. *Inorg. Chem.* **1963**, *2*, 917. (b) Diebler, H.; Sutin, N. *J. Phys. Chem.* **1964**, *68*, 174. (c) Wilkins, R. G.; Yelin, R. E. *Inorg. Chem.* **1968**, *7*, 2667.

(12) (a) Wong, C. L.; Kochi, J. K. *J. Am. Chem. Soc.* **1979**, *101*, 5593. (b) Fukuzumi, S.; Wong, C. L.; Kochi, J. K. *Ibid.* **1980**, *102*, 2928.

(13) Howell, J. O.; Goncalves, J.; Amatore, C.; Klasinc, L.; Wightman, R. M.; Kochi, J. K. *J. Am. Chem. Soc.* **1984**, *106*, 3968.

(14) Schlesener, C. J.; Amatore, C.; Kochi, J. K. *J. Am. Chem. Soc.* **1984**, *106*, 3567.

(15) Marcus, R. A. *J. Chem. Phys.* **1956**, *24*, 4966; **1965**, *43*, 679.

(16) Rollick, K. L.; Kochi, J. K. *J. Am. Chem. Soc.* **1982**, *104*, 1319.

† Present address: Department of Chemistry, University of Houston, University Park, Houston, TX 77004.

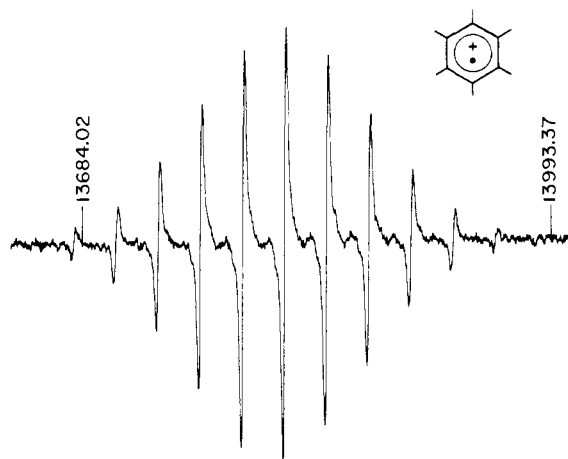
via a similar outer-sphere mechanism.

The rate of the intervening step in eq 6 involving proton loss from the methylbenzene cation radical is uncertain.¹⁷ Since methylbenzene cation radicals can only be observed as transient intermediates, it is generally conceded that proton loss is very rapid and irreversible. For example, the inability to observe the cation radical of hexamethylbenzene when it was produced electrochemically at $-40\text{ }^\circ\text{C}$ in acetonitrile by cyclic voltammetry or double-step chronoamperometry led Parker and co-workers¹⁸ to the conclusion that its lifetime must be $<10^{-4}\text{ s}$. On the other hand, Bewick et al.¹⁹ have reported a value of $\sim 700\text{ s}^{-1}$ for the disappearance of hexamethylbenzene cation radicals in the same medium, based on their use of transient electrochemical techniques including linear sweep voltammetry, chronoamperometry, chronocoulometry, and spectroelectrochemistry.

The measurement of the rates of deprotonation from methylbenzene cation radicals offers a unique opportunity to examine structural effects on proton loss from a carbon center of a transient acid. It also presents a challenge commonly encountered in chemical kinetics to extract the experimental rate constant of a step following a partially reversible preequilibrium.²⁰ [Such a kinetics situation in electrochemistry is described by the ubiquitous ECE process.] In this study, we wish to present a kinetics method for the determination of the proton-transfer rate constant k_2 based on our studies of aromatic oxidation.

Results

The formation of aromatic cation radicals as transient intermediates in eq 5 is shown by the ESR spectrum obtained when a methylarene such as hexamethylbenzene is simply mixed with tris(phenanthroline)iron(III), hereafter referred to either as FeL_3^{3+} or Fe(III) .



For the deprotonation studies we chose the series of methylbenzene cations radicals derived from the polymethylated analogues ArCH_3 = hexamethylbenzene, pentamethylbenzene, durene, prehnitene, and isodurene.

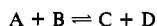
Description of the Kinetics Method. We previously observed two experimental situations which describe the kinetics of aromatic oxidative substitution by FeL_3^{3+} in acetonitrile solutions containing pyridine bases.¹⁴ At one extreme of suitably high concentrations of base, the disappearance of iron(III) followed first-order kinetics

(17) However, for a theoretical study of proton transfer from methylarene cation radicals based on thermochemical calculations, see: Ebersson, L.; Jönsson, L.; Wistrand, L.-G. *Acta Chem. Scand., Ser. B* **1978**, *B32*, 520.

(18) Berek, J.; Ahlberg, E.; Parker, V. D. *Acta Chem. Scand., Ser. B* **1980**, *B34*, 85.

(19) Bewick, A.; Mellor, J. M.; Pons, B. S. *Electrochim. Acta* **1980**, *25*, 931.

(20) In essence, such a kinetics behavior arises whenever a second-order equilibrium is followed by an irreversible reaction, i.e.



Although such a mechanism is likely to be commonly encountered it is not usually treated, in contrast to the analogous case involving a first-order equilibrium.

when the methylarene was in excess, i.e.

$$\ln \frac{[\text{Fe(III)}]}{[\text{Fe(III)}]_0} = -k_e t \quad (8)$$

where $[\text{Fe(III)}]_0$ and $[\text{Fe(III)}]$ represent the concentrations of FeL_3^{3+} initially and at time t , respectively. At the other extreme of low concentrations of base (but $[\text{B}]$ and $[\text{ArCH}_3]$ in excess of $[\text{FeL}_3^{3+}]$), the disappearance of iron(III) obeyed a more complex dependence given in eq 9.

$$\ln \frac{[\text{Fe(III)}]}{[\text{Fe(III)}]_0} - \frac{[\text{Fe(III)}]}{[\text{Fe(III)}]_0} + 1 = -k_e t \quad (9)$$

Indeed the experimental rate expressions in eq 8 and 9 both stem from the general rate law derived from Scheme II and expressed as

$$\left\{ 1 + \frac{k_{-1}[\text{Fe(III)}]_0}{k_2[\text{py}]} \right\} \left\{ \ln \frac{[\text{Fe(III)}]}{[\text{Fe(III)}]_0} \right\} + \left\{ \frac{k_{-1}[\text{Fe(III)}]_0}{k_2[\text{py}]} \right\} \left\{ 1 - \frac{[\text{Fe(III)}]}{[\text{Fe(III)}]_0} \right\} = -2k_1[\text{ArCH}_3]_0 t \quad (10)$$

by considering the steady-state behavior of $[\text{ArCH}_3^{\cdot+}]$ and $[\text{ArCH}_2^{\cdot}]$. (For the derivation of the rate law, see the Experimental Section.) Equations 8 and 9 then represent a pair of limiting situations in which the kinetics are determined by the rate of the back electron transfer in eq 5 relative to that of the deprotonation step in eq 6. For convenience, we evaluate these relative rate processes by the constant parameter p ,²¹ i.e.

$$p = \frac{k_{-1}[\text{Fe(III)}]_0}{k_2[\text{B}]} \quad (11)$$

At one limiting extreme of high base concentrations when $p \ll 1$ (i.e., the rate of deprotonation is faster than back electron transfer), it follows from eq 10 that the experimental rate constant k_e in eq 8 is simply the pseudo-first-order rate constant $k_e = 2k_1[\text{ArCH}_3]_0$. At the other limiting extreme of low base concentrations when $p \gg 1$, it can also be readily shown from eq 10 that the experimental rate constant in eq 9 is $k_e = 2k_1[\text{ArCH}_3]_0/p$. Chemically, this limit represents electron transfer in full equilibrium followed by rate-limiting deprotonation of the methylbenzene cation radical. As such, it should allow the deprotonation rate constants to be measured simply from the variation of the rate as a function of the base concentration. Unfortunately we found this straightforward procedure to be difficult in practice to implement uniformly.²² Thus we generally observed (at the requisite low concentrations of base) a kinetics behavior which was actually intermediate between the limiting extremes described by eq 8 and 9. In other words, we could not practically achieve a kinetics situation in which the rate was solely limited by deprotonation without admixture from an electron-transfer component.

Let us therefore return to the primary rate law in eq 10 and reexpress it more clearly in a two-parameter form, i.e.

$$\ln \frac{[\text{Fe(III)}]}{[\text{Fe(III)}]_0} + \gamma \left\{ 1 - \frac{[\text{Fe(III)}]}{[\text{Fe(III)}]_0} \right\} = \frac{-2k_1[\text{ArCH}_3]_0}{1+p} t \quad (12)$$

where $\gamma = p/(1+p)$. The parameter γ is most conveniently thought of as the measure of how close a particular system is to one of the limiting extremes, i.e., $\lim_{\gamma \rightarrow 0}(\text{eq 12}) = \text{eq 8}$ and $\lim_{\gamma \rightarrow 1}(\text{eq 12}) = \text{eq 9}$.

The task thus directly resolves into one of finding the best value of the factor γ in order to linearize the data set relating to $[\text{Fe(III)}]/[\text{Fe(III)}]_0$ on the left side of eq 12 with time. In practice,

(21) The back electron transfer is actually given by $2xk_{-1}[\text{Fe(III)}]_0$, where $2x$ is the extent of reaction (i.e., $[\text{Fe(II)}]/[\text{Fe(III)}]_0$) and constant at a given time.

(22) The adjustment of the base concentration to observe reliably the kinetics according to eq 9 proved to be experimentally difficult. Thus for some methylarene/pyridine pairs even the lowest concentration of base considered to be possible (i.e., $[\text{py}] = 10[\text{Fe(III)}]_0$) resulted in a mixed kinetic behavior.

Table I. Measured Values of the Electron-Transfer Rate Constant k_1 and the Rate Constant Ratio k_{-1}/k_2 for Hexamethylbenzene Obtained with Various Substituted Pyridines^a

no.	x	$k_1, M^{-1} s^{-1}$	$(k_{-1}/k_2), \times 10^{-3}$	no.	x	$k_1, M^{-1} s^{-1}$	$(k_{-1}/k_2), \times 10^{-3}$
1	2-fluoro	<i>b</i>	410 (60)	8	2-methyl	12 (1)	0.25 (0.03)
2	2-chloro	<i>b</i>	55 (5)	9	4-methyl	16 (2)	0.34 (0.10)
3	3-cyano	13 (2)	32 (4)	10	4-methoxy	22 (8)	0.37 (0.20)
4	4-cyano	14 (5)	18 (6)	11	2,6-dimethyl	14 (4)	0.32 (0.08)
5	3-chloro	15 (2)	6.6 (0.9)	12	2,6-di- <i>tert</i> -butyl	<i>b</i>	40 (4)
6	3-fluoro	15 (2)	6.1 (1.1)	13	2,4,6-trimethyl	13 (1)	0.14 (0.02)
7	hydrogen	13 (3)	0.67 (0.24)				

^a Determined in acetonitrile solution containing 0.10 mM Fe(phen)₃(PF₆)₃ and 0.1 M LiClO₄ at 22 °C. Values in parentheses indicate one standard deviation. ^b Since the kinetics followed the limiting situation in eq 9, the value of $k_1 = 14 M^{-1} s^{-1}$ was assumed in order to extract the values of k_{-1}/k_2 from the measured k_a .

Table II. Measured Values of the Electron-Transfer Rate Constant k_1 and the Rate Constant Ratio k_{-1}/k_2 for Various Methylbenzenes and Substituted Pyridines^a

x	no.	$(k_{-1}/k_2), \times 10^{-3}$		$(k_{-1}/k_2), \times 10^{-3}$		$(k_{-1}/k_2), \times 10^{-3}$		$(k_{-1}/k_2), \times 10^{-3}$				
		k_1	$(k_{-1}/k_2), \times 10^{-3}$	no.	$k_1, \times 10^2$	$(k_{-1}/k_2), \times 10^{-3}$	no.	$k_1, \times 10^3$	$(k_{-1}/k_2), \times 10^{-3}$	no.	$k_1, \times 10^2$	$(k_{-1}/k_2), \times 10^{-2}$
4-cyano	14	0.23 (0.01)	6.3 (0.3)	18	2.5 (0.6)	5.5 (2.2)	22	4.5 (1.4)	6.2 (3.1)	26	4.0 (0.1)	510 (60)
3-chloro	15	0.30 (0.03)	3.3 (0.5)	19	3.6 (1.4)	3.8 (1.8)	23	4.1 (1.2)	2.4 (1.1)	27	6.0 (4.0)	190 (230)
hydrogen	16	0.24 (0.01)	0.36 (0.09)	20	3.4 (0.3)	0.23 (0.09)	24	6.3 (0.9)	0.43 (0.13)	28	5.8 (1.7)	0.79 (0.70)
2,6-dimethyl	17	0.33 (0.03)	0.14 (0.01)	21	2.6 (0.4)	0.055 (0.036)	25	5.5 (0.9)	0.071 (0.044)	29	2.8 (1.2)	0.39 (0.19)

^a Determined in acetonitrile solution containing 0.1 mM Fe(phen)₃(PF₆)₃ and 0.1 M LiClO₄ at 22 °C. The second-order rate constants are given in units of $M^{-1} s^{-1}$. Values in parentheses indicate one standard deviation.

a computer program for multiple linear regression was used to solve for the coefficients k_a^{-1} and γk_a^{-1} in the rearranged form of eq 12, i.e.

$$-k_a^{-1} \ln \left(\frac{[\text{Fe(III)}]}{[\text{Fe(III)}]_0} \right) - \gamma k_a^{-1} (1 - [\text{Fe(III)}]/[\text{Fe(III)}]_0) = t \quad (13)$$

where $k_a = 2k_1[\text{ArCH}_3]_0/(1+p)$. (See the Experimental Section for important details of the data treatment.) The efficacy of this method is shown by the linearity of the central line III in Figure 1 for a representative kinetics run. By contrast, the upper line I describes the same data as a convex curve when plotted as a function of the limiting situation described in eq 8; the lower line II describes the data as a concave curve when plotted as a function of the other limiting situation described in eq 9. The regression coefficients k_a^{-1} and γ obtained in this manner lead directly to values of the electron-transfer rate constant k_1 and the ratio of rate constants k_{-1}/k_2 via the parameter p in eq 11. The experimental values of these rate constants for hexamethylbenzene obtained with a wide variety of ring-substituted pyridine bases are tabulated in Table I.

The validity of the kinetics method based on eq 13 is revealed in several important ways by the results in Table I. First, the values of the rate constant k_1 listed in the third and seventh columns are found to be invariant with the structure of the pyridine base, as it must be for the electron-transfer process in eq 5 (Scheme II) involving a common substrate (i.e., hexamethylbenzene). Second, the values of the rate-constant ratio k_{-1}/k_2 in the fourth and eighth columns are strongly dependent on the structure of the pyridine base. Since the back electron transfer rate constant k_{-1} (like the forward rate constant k_1) will be constant for hexamethylbenzene, the variations in the ratio k_{-1}/k_2 must directly reflect changes in the deprotonation rate constant k_2 with the pyridine base. Indeed we observe the decreasing trend in k_{-1}/k_2 by a factor of 3000 from 2-fluoropyridine to α -collidine to parallel the increasing trend in base strengths of the substituted pyridines. The outstanding exception is the highly sterically hindered base, 2,6-di-*tert*-butylpyridine for which the value of k_{-1}/k_2 is comparable to those of the significantly weaker bases 2-chloro- and 3-cyanopyridine.

The foregoing conclusions regarding the values of k_1 and k_{-1}/k_2 for hexamethylbenzene and the various pyridine bases also applies

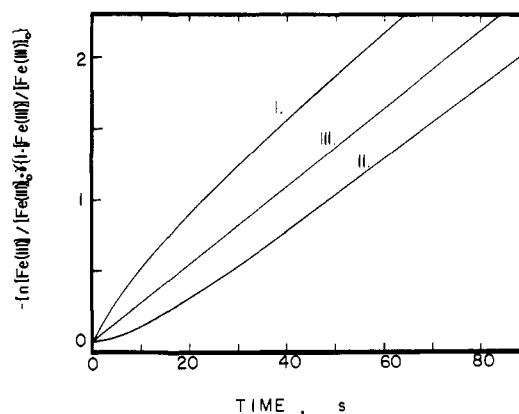
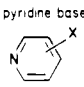
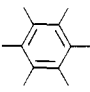
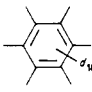
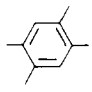
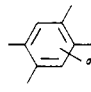


Figure 1. Kinetics of the oxidative substitution of 3.2 mM hexamethylbenzene by 0.112 mM FeL₃³⁺ in acetonitrile containing 31 mM pyridine and 0.1 M LiClO₄ at 22 °C plotted as a function of $-\ln([\text{Fe(III)}]/[\text{Fe(III)}]_0) - \gamma(1 - [\text{Fe(III)}]/[\text{Fe(III)}]_0)$ according to eq 8 ($\gamma = 0$, curve I), eq 9 ($\gamma = 1$, curve II), and eq 13 ($0 < \gamma < 1$, curve III).

to the other methylarenes examined in this study, i.e., pentamethylbenzene, durene, and prehnitene. Thus the results in the third, sixth, and ninth columns of Table II show that the electron-transfer rate constants k_1 for a given methylarene do not vary with the different pyridine bases if they are considered within the experimental error limits which are evaluated in the parentheses. Moreover, the trend in the values of the rate constant ratio k_{-1}/k_2 for every methylarene decreases in the same way in proceeding from the weak (4-cyanopyridine) to the stronger (2,6-lutidine) pyridine base.

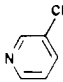

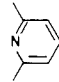
The kinetic isotope effect was examined by comparing the rates of hexamethylbenzene with those of the perdeuterated HMB-*d*₁₈, and the rates of durene with those of the completely methyl-deuterated derivative DUR-*d*₁₄. The results listed in columns 2/4 and 6/8 of Table III show that the electron-transfer rate constant k_1 is not subject to a deuterium kinetic isotope effect. This provides further compelling support for the validity of kinetics method in eq 13 to provide reliable values of k_1 (and k_{-1}/k_2), since the ionization potentials of HMB and HMB-*d*₁₈ as well as DUR and DUR-*d*₁₄ are the same.²³ By contrast, the rate constant ratios

Table III. Kinetic Isotope Effect for the Deprotonation of Hexamethylbenzene and Durene Cation Radicals^a

pyridine base 								
	k_1	$(k_{-1}/k_2), \times 10^{-2}$	k_1	$(k_{-1}/k_2), \times 10^{-2}$	$k_1, \times 10^2$	$(k_{-1}/k_2), \times 10^{-2}$	$k_1, \times 10^2$	$(k_{-1}/k_2), \times 10^{-2}$
4-cyano	14 (5)	180 (60)	<i>b</i>	800 (30)				
3-chloro	15 (2)	66 (9)	<i>b</i>	310 (10)	3.6 (1.4)	38 (18)	4.0 (1.0)	160 (50)
hydrogen	13 (3)	6.7 (2.4)	15 (4)	22 (5)	3.4 (0.3)	2.3 (0.9)	4.0 (0.1)	7.1 (0.6)
2,6-dimethyl	14 (4)	3.2 (0.8)	13 (3)	12 (2)				

^a In acetonitrile solution containing 0.1 mM Fe(phen)₃(PF₆)₃ and 0.1 M LiClO₄ at 22 °C. Values in parentheses indicate one standard deviation. ^b In these runs, the kinetics afforded the limiting situation in eq 9 and k_1 could not be independently extracted. Values of k_{-1}/k_2 were obtained from k_e using values of k_1 determined for HMB-*d*₀.

Table IV. Salt Effect on the Deprotonation Rate Constants for Hexamethylbenzene Cation Radical with Various Pyridine Bases^a

salt, ^b M						
	k_1	$(k_{-1}/k_2), \times 10^{-3}$	k_1	$(k_{-1}/k_2), \times 10^{-1}$	k_1	$(k_{-1}/k_2), \times 10^{-1}$
none	28 (1) ^c	0.77 (0.09)	28 (1) ^c	9.7 (0.4)	29 (2) ^c	4.2 (1.2)
TEAP (0.1)	12 (1)	5.2 (0.7)	12 (2)	35 (7)	13 (2)	29 (6)
TBAP (0.1)	<i>d</i>	8.5 (0.1)	15 (1)	50 (2)	17 (2)	41 (4)
LiClO ₄ (0.1)	15 (2)	6.6 (0.9)	13 (3)	67 (24)	14 (4)	32 (8)

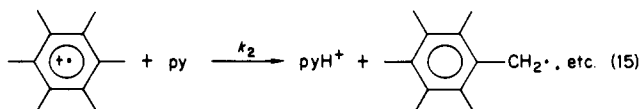
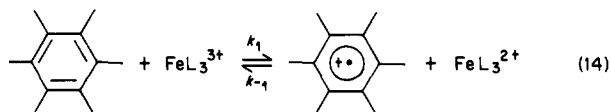
^a In acetonitrile containing 0.1 mM Fe(phen)₃(PF₆)₃ at 22 °C. Values in parentheses indicate one standard deviation. ^b TEAP = tetraethylammonium perchlorate, TBAP = tetra-*n*-butylammonium perchlorate. ^c Compare with a value of 39 M⁻¹ s⁻¹ reported in ref 14. ^d Kinetics followed the limiting situation in eq 9, and the value of $k_1 = 14$ M⁻¹ s⁻¹ was used to extract k_{-1}/k_2 from k_e .

k_{-1}/k_2 of the deuterated derivative are significantly larger than those of the parent methylarene. Since the back electron transfer rate constant k_{-1} is the same for each pair (vide supra), the deuterium kinetic isotope effects observed in k_{-1}/k_2 must arise exclusively from the decreases in the deprotonation rate constants k_2 upon deuteration of the methyl groups.

The salt effect was examined by treating hexamethylbenzene with Fe(phen)₃³⁺ and various pyridine bases in acetonitrile solutions which either had no added salt or contained 0.10 M lithium perchlorate, tetraethylammonium perchlorate (TEAP), or tetra-*n*-butylammonium perchlorate (TBAP). The kinetics analysis with the aid of eq 13 showed that the electron-transfer rate constant k_1 decreased very slightly in the presence of added salt by an amount which was invariant with the nature of the cation, as tabulated in columns 2, 4, and 6 of Table IV. By contrast, the added salt led to an increase in the rate constant ratio k_{-1}/k_2 by an amount (~4–9-fold) which depended on the pyridine base strength and to a lesser extent on the cation structure (see columns 3, 5, and 7 of Table IV). Such a change corresponds to a significant negative salt effect on only the deprotonation rate constant k_2 .

Discussion

Electron transfer from various methylbenzenes can be effectively achieved with the coordinatively saturated iron(III) complex FeL₃³⁺, where L = 1,10-phenanthrolines. The methylbenzene cation radicals formed in this way are sufficiently acidic to undergo proton transfer to various pyridines py, e.g.



A rigorous analysis of the kinetics shows the electron transfer in eq 14 to be reversible, and the rate of back electron transfer to be competitive with proton loss in eq 15. As such, we identify this competition and define it as a rate ratio $p = k_{-1}/k_2$.

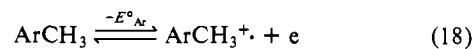
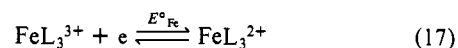
(23) The data for hexamethylbenzene are included in ref 13; that for durene is unpublished.

(II)]₀/k₂[B] which determines the extent to which the overall rate is governed by electron transfer or proton loss from the methylbenzene cation radical. The complete solution of the experimental kinetics according to eq 12 affords accurate values of two independent parameters: the electron-transfer rate constant k_1 and the rate ratio p , which is in turn directly related by eq 11 to the rate-constant ratio k_{-1}/k_2 at a particular value of [Fe(II)]₀ and [py]. The validity of the kinetics analysis to afford reliable values of k_1 and k_{-1}/k_2 , as tabulated in Tables I and II, can be demonstrated in three different ways. First, the electron-transfer rate constants k_1 obtained by this method are the same as those previously measured under quite different conditions in which electron transfer was solely rate limiting.¹⁴ [Compare eq 8 which is valid at high concentrations of the pyridine bases.] Second, the values of the rate constant k_1 in Tables I and II are found to be independent of the concentration and the structure of the pyridine base, in accord with the electron-transfer step which precedes proton loss. Third, despite the large differences in overall reactivity of hexamethylbenzene and its perdeuterated derivative, the values of k_1 evaluated by the kinetics method are the same. [Note the ionization potential IP and oxidation potential E°_{Ar} of HMB and HMB-*d*₁₈ are equal to within ±0.02 V].

Kinetic Acidity of Methylbenzene Cation Radicals. The availability of independent values of the electron-transfer rate constant k_1 and the rate constant ratio k_{-1}/k_2 allows us now to evaluate the absolute magnitudes of the rate constant k_2 for the deprotonation of various methylbenzene cation radicals by pyridine bases. Thus the equilibrium constant K_{et} for the electron transfer preceding proton transfer is simply given by the usual equilibrium relationship, i.e.

$$K_{\text{et}} = k_1/k_{-1} = \exp(\mathcal{F}\Delta E/RT) \quad (16)$$

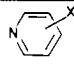
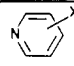
where $\Delta E = E^\circ_{\text{Fe}} - E^\circ_{\text{Ar}}$ represents the difference between standard reduction potentials of the iron(III) complex FeL₃³⁺ and the methylarene, i.e.



Furthermore the measured values of k_1 and k_{-1}/k_2 listed in Tables I and II can be reexpressed as a normalized rate constant ratio, i.e.

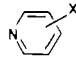
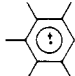
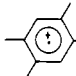
$$\kappa = k_2 k_1 / n k_{-1} \quad (19)$$

Table V. Kinetic Acidity of Hexamethylbenzene Cation Radical with Various Substituted Pyridine Bases^a

no.		pK_a^b	$\log \kappa$	$\log k_2$	no.		pK_a^B	$\log \kappa$	$\log k_2$
1	2-fluoro	4.2 ^b	-5.23	2.56	8	2-methyl	14.0	-2.09	5.69
2	2-chloro	6.3	-4.36	3.42	9	4-methyl	14.3	-2.11	5.67
3	3-cyano	7.0 ^b	-4.16	3.62	10	4-methoxy	15.0 ^b	-2.01	5.77
4	4-cyano	8.0	-3.89	3.89	11	2,6-dimethyl	15.4	-2.14	5.64
5	3-chloro	9.0	-3.42	4.36	12	2,6-di- <i>tert</i> -butyl	11.8 ^b	-4.23	3.55
6	3-fluoro	9.4 ^b	-3.38	4.40	13	2,4,6-trimethyl	16.8	-1.79	5.99
7	hydrogen	12.3	-2.49	5.29					

^a The value of $\kappa = k_2 k_1 / n k_{-1}$ from Table I and is normalized for the number n of methyl substituents. For the redox equilibrium ΔE° , the value of $E^\circ_{Fe} = 1.09$ V was used together with estimated values of E°_{Ar} , as described in the Experimental Section. ^b Estimated from the correlation of [pK_a^B] in acetonitrile and water as described in the Experimental Section.

Table VI. Kinetic Acidities of Methylbenzene Radical Cations Evaluated from the Estimates of the Redox Equilibrium^a

	no.	$\log \kappa$	$\log k_2$		no.	$\log \kappa$	$\log k_2$		no.	$\log \kappa$	$\log k_2$
4-cyano	14	-5.14	4.87	18	-5.95	5.08	22	-6.74	5.31		
3-chloro	15	-4.74	5.27	19	-5.62	5.41	25	-6.37	5.68		
hydrogen	16	-3.88	6.13	20	-4.43	6.60	24	-5.44	6.61		
2,6-dimethyl	17	-3.33	6.68	21	-3.93	7.10	25	-4.71	7.34		

^a The value of $\kappa = k_2 k_1 / n k_{-1}$ from Table I and is normalized for the number n of methyl substituents. For the redox equilibrium ΔE° , the value of $E^\circ_{Fe} = 1.09$ V was used together with estimated values of E°_{Ar} , as described in the Experimental Section.

where n is the number of acidic methyl protons in the cation radical.²⁴ The values of κ derived in this manner for hexamethylbenzene and various pyridine bases are presented in Table V. The combination of eq 19 with eq 16 affords the deprotonation rate constants k_2 for hexamethylbenzene cation radical simply in terms of the experimental κ and the redox equilibrium.

Although the standard reduction potential E°_{Fe} of $Fe(phen)_3^{3+}$ is readily determined,¹¹ that E°_{Ar} of hexamethylbenzene is unfortunately not available in acetonitrile. However, the values of E°_{Ar} in this medium can be evaluated by several indirect procedures described in the Experimental Section. Using this estimate of E°_{Ar} and the experimentally determined values of κ , we computed from eq 19 the values of the rate constants k_2 for the deprotonation of hexamethylbenzene cation radical by various pyridine bases. It is noteworthy that these deprotonation rate constants in Table V range from $\sim 4 \times 10^2$ M⁻¹ s⁻¹ for the weakest base 2-fluoropyridine to more than 9×10^5 M⁻¹ s⁻¹ for the strongest base 2,4,6-trimethylpyridine examined in this system.²⁵

The same procedure was used to determine the deprotonation rate constants for the cation radicals derived from pentamethylbenzene, durene, and prehnitene. The results are summarized in Table VI.²⁶

Free Energy Relationships for Proton Transfer Using the Brønsted Law. The availability of the deprotonation rate constants for various methylarene cation radicals by different pyridine bases encourages us to develop a free energy relationship for proton transfer. According to the Brønsted catalysis law, the rate constants k_2 for proton transfer in a series of related acid-base pairs may be treated as a function of the equilibrium constant K_a for reversible proton exchange.²⁷

$$k_2 = G(K_a)^\alpha \quad (20)$$

(24) Such a simple normalization procedure does not take into account the differences in reactivity of the inequivalent methyl groups present in pentamethylbenzene and prehnitene.

(25) (a) Note many of the values of pK_a^B in Table V refer to the acid dissociation constants of the pyridinium ions determined directly measured in acetonitrile solution by: Cauquis, G.; Deronzier, A.; Serve, D.; Viell, E. *J. Electroanal. Chem. Interfacial Electrochem.* **1975**, *60*, 205. (b) Others were obtained from a correlation of the pK_a^B value in water [Perrin, D. D.; Dempsey, B.; Serjeant, E. P. "pK_a Prediction from Organic Acids and Bases"; Chapman and Hall: London, 1981] with that in acetonitrile (vide supra). (c) The value for 2,6-di-*tert*-butylpyridine was from: Brown, H. C.; Kanner, B. *J. Am. Chem. Soc.* **1966**, *88*, 986 determined with others in 50% aqueous ethanol, and correlated against those in water.

(26) Since isodurene has three quite inequivalent methyl groups, the value of n in eq 19 is difficult to assign,²⁴ and κ was not computed.

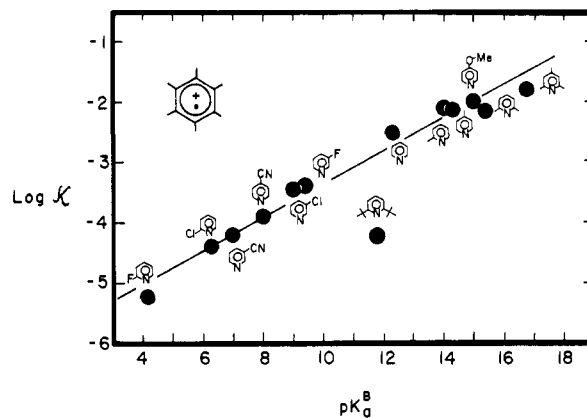


Figure 2. Brønsted relationship for the rates of deprotonation of hexamethylbenzene cation radical by various pyridine bases. The line representing the Brønsted slope $\alpha = 0.26$ has a correlation coefficient 0.99 excluding the datum for 2,6-di-*tert*-butylpyridine.

A. Hexamethylbenzene Cation Radical and Various Pyridine Bases. Let us first consider the rates of proton transfer from hexamethylbenzene cation radical to a series of substituted pyridines whose base strengths are indicated by their values of [pK_a^B]. Under these circumstances, it follows from eq 19 that the rates of proton transfer ($\log k_2$) are directly related to our experimental measure κ , i.e.

$$\log k_2 = \log(n\kappa) - \mathcal{F}\Delta E / (RT \ln 10) \quad (21)$$

since the contribution ΔE° from the redox preequilibrium will be invariant. Accordingly, the plot of $\log \kappa$ against the pyridine base strengths [pK_a^B] shown in Figure 2 represents the Brønsted relationship

$$\log \kappa = \alpha[pK_a^B] + C \quad (22)$$

where the constant C includes the redox equilibrium $\mathcal{F}\Delta E/RT \ln 10$ as well as $\log G$. Indeed this linear free energy relationship accommodates all the rate data for the deprotonation of hexamethylbenzene cation radical by various pyridine bases with one striking exception. Clearly, the behavior of the highly sterically

(27) (a) Bell, R. P. "The Proton in Chemistry", 2nd ed.; Cornell University Press: Ithaca, NY, 1973. (b) Caldin, E., Gold, V., Eds. "Proton Transfer Reactions"; Chapman and Hall: London, 1975.

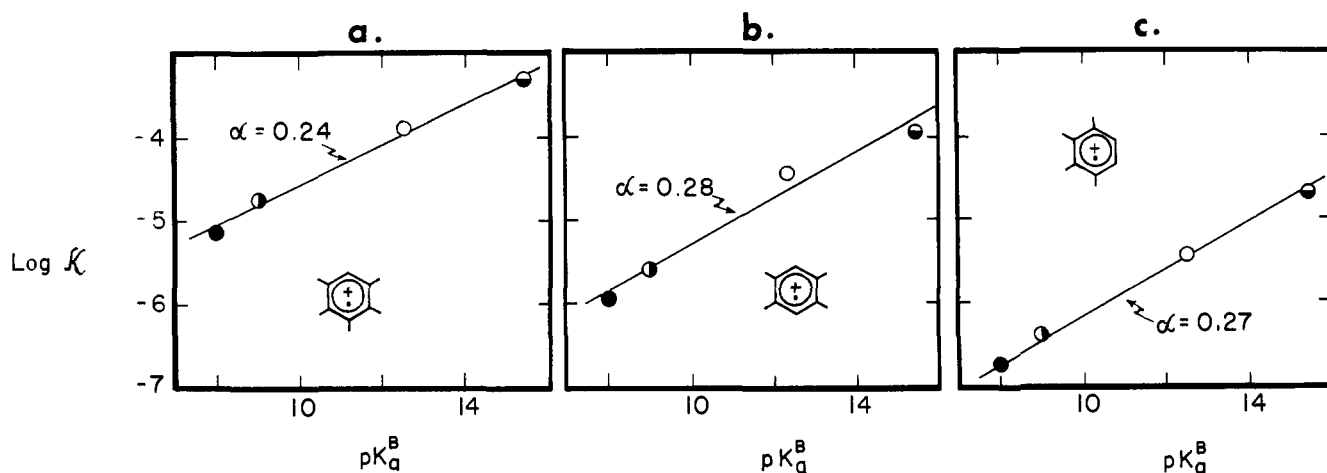


Figure 3. Brønsted relationship for the rates of deprotonation of the cation radicals of (a) pentamethylbenzene, (b) durene, and (c) prehnitene with a common series of pyridine bases: (●) 4-cyanopyridine, (◐) 3-chloropyridine, (○) pyridine, and (◑) lutidine.

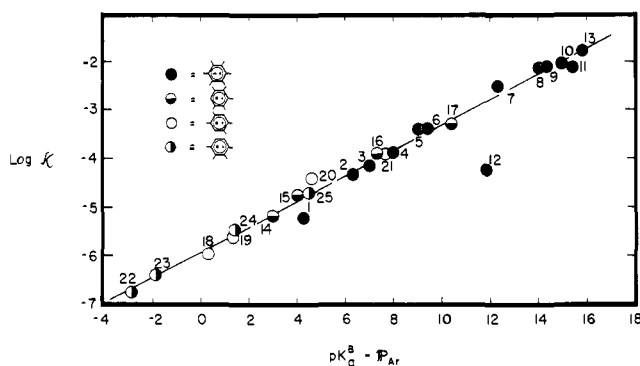


Figure 4. General Brønsted relationship for the rates ($\log \kappa$) of proton loss for methylbenzene cation radicals (hexamethylbenzene (●), pentamethylbenzene (◐), durene (○), and prehnitene (◑)) by various pyridine bases as a function of the base strength [pK_a^B] and the contribution P_{Ar} from the acidity of $ArCH_3^+$. The methylarene cation radical/pyridine (acid-base) pairs are identified by numbers in Tables V and VI.

hindered 2,6-di-*tert*-butylpyridine is deviant, it being at least an order of magnitude less effective in proton removal from HMB^+ than expected merely on the basis of its base strength. Otherwise the Brønsted correlation applies well to other ortho-substituted and ortho,ortho'-disubstituted pyridines (see especially the series of methylated derivatives α -picoline, α -lutidine, and α -collidine included in Figure 2), as indicated by the correlation coefficient of 0.99.

B. Unified Brønsted Correlation for Proton Transfer. The series of structurally related methylbenzene cation radicals and substituted pyridine bases in Table VI together with the rate data for hexamethylbenzene cation radical in Table V permit an examination of a unified free energy relationship for proton transfer at a highly labile carbon center.

We proceed by noting that the Brønsted relationship in eq 22 also applies to the other methylarenes examined in this study. Thus Figure 3 illustrates the linear correlation of the experimental rate measure $\log \kappa$ of three methylarenes with a common series of pyridine bases.²⁸ It is noteworthy that the slope α in each of the graphs is 0.26 ± 0.02 , which is the same as that for hexamethylbenzene in Figure 2.

These common slopes indicate that all the data which are contained in Figures 2 and 3 will be accommodated in a *single figure*, if each graph is displaced along the abscissa by an amount P_{Ar} which depends on the particular methylarene cation radical. The results of this operation are shown in Figure 4, in which the line represents a least-squares correlation of all the data with a

(28) The Brønsted plot for isodurene (assuming $n = 4$ in eq 19²⁶) was considerably different from that of the other methylarenes [i.e., $\alpha = 0.45$, correlation coefficient 0.97.] It thus is not considered further.

Table VII. Relative Values of [pK_a^A] for Various Methylbenzene Cation Radicals^a

$ArCH_3^+$	P_{Ar}	$\Delta E^\circ_{rel}{}^b$	$[\Delta pK_a^A]^c$
	0.0	0.0	0.0
	5.0 (0.5)	0.14 (0.07)	-3.7
	7.7 (0.9)	0.20 (0.03)	-5.7
	10.9 (1.1)	0.26 (0.03)	-5.5

^a The numbers in parentheses represent one standard deviation. ^b The value in volts of the potential ΔE° for the redox equilibrium relative to that of hexamethylbenzene. ^c Note that an error of ~ 30 mV in ΔE° (see column 3) is sufficient to alter the ΔpK_a^A value by 2 units.

correlation coefficient of 0.99.²⁹ Thus the empirical free energy relationship in Figure 4 which is generally applicable to all methylarenes and pyridine bases can be expressed as

$$\log \kappa = \alpha[pK_a^B - P_{Ar}] + C \quad (23)$$

It also follows from the general Brønsted catalysis law of eq 20 that the correlation in Figure 3 represents the relationship

$$\log \kappa = \alpha[pK_a^B - pK_a^A] + \frac{\mathcal{F}\Delta E}{RT \ln 10} + \text{constant} \quad (24)$$

where [pK_a^A] is the acidity constant of the methylarene cation radical. In other words, the contribution P_{Ar} arising from different methylarenes in Figure 4 actually represents the acidities of their cation radicals, i.e.

$$P_{Ar} = [\Delta pK_a^A] - \Delta E^\circ / 0.059\alpha \quad (25)$$

where [ΔpK_a^A] and ΔE° are the acidity constant and oxidation potential, respectively, of a particular $ArCH_3^+$ relative to that of HMB^+ , taken as a reference, and the value of $\mathcal{F}/(RT \ln 10)$ is 0.059 at 25 °C.

C. The Acidities of Methylarene Cation Radicals. The formulation in eq 25 emphasizes that the thermodynamic acidities [pK_a^A] of the entire series of methylarenes can be obtained from

(29) In practice, a computer program for multiple linear regression was used to evaluate the values of α and P_{Ar} by considering all the data in Tables V and VI.

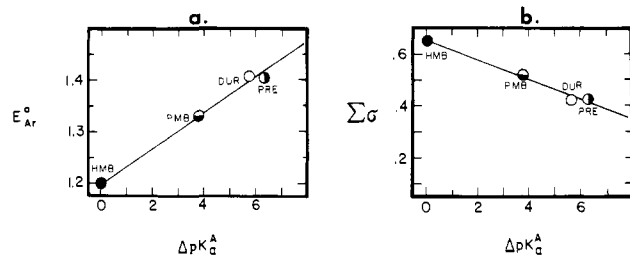


Figure 5. Structural effects of methylarenes on the relative acidities [ΔpK_a^A] of the cation radicals. Relationship with (a) the standard oxidation potentials E°_{Ar} in trifluoroacetic acid and (b) the Hammett substituent constants $\Sigma\sigma$.

kinetic measurements of iron(III) oxidation, merely from the knowledge of ΔE° and the acidity of a particular reference (e.g., hexamethylbenzene). We stress the caveat, however, that the values of the acidity obtained by the kinetics technique are strongly dependent on the accuracy of the potential measurements ΔE° from the redox equilibrium. For example, an error as small as 16 mV is sufficient to cause a unit change in [pK_a^A] of a methylarene cation radical, since the value of $\alpha = 0.26$ is applicable in eq 25.

The values of P_{Ar} for several methylbenzene cation radicals evaluated according to eq 25 are listed in the second column of Table VII. Owing largely to the experimental necessity of indirect measures for E°_{Ar} (see Table XI, Experimental Section), the potential measurements for the redox preequilibrium in the third column are not presently of sufficient reliability to allow accurate values of [ΔpK_a^A] to be determined. With this limitation in mind, the best values of [ΔpK_a^A] for the methylarene cation radicals listed in column 4 should be accepted to one significant figure.

The relative acidities of the various methylarene cation radicals can be viewed in two ways. Thus the relationship of [ΔpK_a^A] with the standard oxidation potential E°_{Ar} of the methylarene in trifluoroacetic acid is shown in Figure 5a.³⁰ A similar relationship with the Hammett substituent constants $\Sigma\sigma$ is shown in Figure 5b.³¹ Both correlations accord with the qualitative notion that the acidity increases with decreasing stability of the cation radical and with decreasing donor property of the methylarene.^{31,32} A long (and highly problematic!) extrapolation in Figure 4 to toluene ($E^\circ_{PhCH_3} = 1.9_3$ V, $\Sigma\sigma = 0.00$) suggests that the pK_a^A of its cation radical is roughly 19 units more negative than that of HMB⁺. Alternatively, it is possible to treat the data according to the thermochemical formulation developed by Arnold and Nicholas, which estimates the pK_a of toluene cation radical to be about 14 units more acidic than that of hexamethylbenzene cation radical.³³

(30) See the data in ref 13.

(31) A weighted average for the Hammett σ values based on $\sigma_{op} = -0.170$ and $\sigma_m = -0.069$ for *o/p*- and *m*-methyl groups, respectively [Gordon, A. J.; Ford, R. A. "The Chemist's Companion"; Wiley: New York, 1972] is computed to be HMB, $\Sigma\sigma = 3\sigma_{op} + 2\sigma_m$; PMB, $\Sigma\sigma = [(2\sigma_{op} + 2\sigma_m) + 2(3\sigma_{op} + \sigma_m) + 2(2\sigma_{op} + 2\sigma_m)]/5$; DUR, $\Sigma\sigma = 2\sigma_{op} + \sigma_m$; PRE, $\Sigma\sigma = 2\sigma_{op} + \sigma_m$. (a) The differences in the values of E°_{Ar} for the methylarenes were assumed to reflect largely the stability of the cation radical in relation to the neutral precursor. (b) For the effect of the methyl groups on the energies of the highest occupied molecular orbitals of the various methylarenes, see ref 32.

(32) Hellbronner, E.; Maier, J. P. In "Electron Spectroscopy"; Brundle, C. R., Baker, A. D., Eds.; Academic Press: New York, 1977; Vol. 1, p 205 ff.

(33) (a) Nicholas, A. M. P.; Arnold, D. R. *Can. J. Chem.* **1982**, *60*, 2165. (b) Using their method 2, eq 24 can be recast in the form:

$$\log \kappa + (\mathcal{F}/RT \ln 10)E^\circ_{AR} = \alpha[pK_a^B + (\mathcal{F}/RT \ln 10)E^\circ_{Ar}] + \text{constant}$$

A plot of the data in Tables V and VI according to this equation indeed affords a linear relationship with a correlation coefficient of 0.95 for the 24 entries (excluding the datum for 2,6-di-*tert*-butylpyridine). Furthermore the slope of $\alpha = 0.28$ is in reasonable agreement with that in Figure 4. If the pK_a^A of toluene cation radical is taken as -12 (as suggested by Nicholas and Arnold), the pK_a^A values of the other aromatic cation radicals are calculated to be: hexamethylbenzene, $+1$; pentamethylbenzene, -1 ; prehnitene, -2 ; isodurene, -2 ; durene, -2 ; hemimellitene, -5 ; pseudocumene, -3 ; mesitylene, -7 ; *p*-, *m*-, and *o*-xylene, -8 , -7 , and -6 based on the recent measurements¹³ of E°_{Ar} . For a discussion of acidity constants in acetonitrile, see: Coetzee, J. F. *Prog. Phys. Org. Chem.* **1967**, *4*, 45.

Table VIII. Kinetic Isotope Effect $k_2(H)/k_2(D)$ for the Deprotonation of Methylarene Cation Radicals by Various Substituted Pyridine Bases^a and Relationship to the Driving Force^b

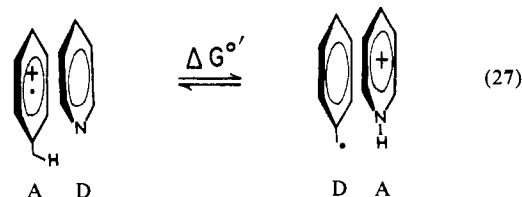
x	ΔpK	$k_2(H)/k_2(D)$	
		ΔpK	$k_2(H)/k_2(D)$
4-cyano	8	4.4	
3-chloro	9	4.7	15
hydrogen	12	3.6	18
2,6-dimethyl	15.5	3.9	2.6

^a From the data in Table III. ^b $\Delta\Delta G^\ddagger = 2.3 RT[\Delta pK]$, where $\Delta pK = pK_a^A - pK_a^B$. An error of ± 0.3 in $k(H)/k(D)$ represents one standard deviation.

The available kinetic data in Tables V and VI also allow the acidities of methylarene cation radicals to be independently evaluated by the Marcus formulation,³⁴ which has previously been used to relate the rates of proton transfer (ΔG^\ddagger) to the driving force $\Delta G^\circ'$ by the expression³⁵

$$\Delta G^\ddagger = w^r + \Delta G^\ddagger_0 \left[1 + \frac{\Delta G^\circ'}{4\Delta G^\ddagger_0} \right]^2 \quad (26)$$

where $\Delta G^\ddagger = -RT \ln(k_2/Z)$, and ΔG^\ddagger_0 is the intrinsic barrier for proton transfer. The driving force $\Delta G^\circ'$ is represented by the composite term $(2.3 RT[pK_a^A - pK_a^B] - w^r + w^p)$, where w^r and w^p are the work terms of the reactants and the products, respectively. Proton transfer between methylarene cation radicals and pyridine bases represents a rather unusual situation insofar as acid-base reactions are concerned. Thus the reactant pair is strikingly akin to the product pair, especially if viewed in terms of charge-transfer interactions shown below.



Thus proton transfer within the encounter complex is accompanied by an interchange of the π -donor (D) and π -acceptor (A) capacities of the methylarene and pyridine moieties on conversion to the successor complex in eq 27.³⁶ As such, we suggest that the magnitudes of the work terms w^r and w^p in this system are comparable. Under these conditions, $\Delta G^\circ' \approx 2.3RT[pK_a^A - pK_a^B]$. Since the Brønsted plot for hexamethylbenzene in Figure 2 shows signs of curvature (compare also Figures 3 and 4), we employed a polynomial regression analysis to fit the experimental curve to the quadratic relationship in eq 26.³⁷ [For details of the computation, see the Experimental Section.] The result was $\Delta G^\ddagger_0 = 6.4$ kcal mol⁻¹, $w^r = 25$ kcal mol⁻¹, and $pK_a^A = 2$. Such magnitudes of ΔG^\ddagger_0 and w^r are indeed reasonable when they are compared with previous reports of these values for other carbon

(34) (a) Marcus, R. A. *J. Phys. Chem.* **1968**, *72*, 891. (b) Cohen, A. O.; Marcus, R. A. *Ibid.* **1968**, *72*, 4249. (c) Marcus, R. A. *J. Am. Chem. Soc.* **1969**, *91*, 7224.

(35) For the application of the Marcus equation to proton transfer, see: (a) Kreevoy, M. M.; Konasewich, D. E. *Adv. Chem. Phys.* **1972**, *21*, 243. (b) Hupe, D. J.; Wu, D. J. *Am. Chem. Soc.* **1977**, *99*, 7653. (c) Kreevoy, M. M.; Oh, S.-W. *Ibid.* **1973**, *95*, 4805. (d) Toullac, J. *Adv. Phys. Org. Chem.* **1982**, *18*, 5.

(36) Arene cation radicals ArH^+ are known to form π -complexes with arenes in the form of dimer cation radicals $[ArH]_2^+$. [See: Edlund, O.; Kinell, P.-O.; Lund, A.; Shimizu, A. *J. Chem. Phys.* **1967**, *46*, 3679. Badger, B.; Brocklehurst, B. *Trans. Faraday Soc.* **1969**, *65*, 2582.] For the structural effects of donor-acceptor complexes between aromatic moieties, see: Foster, R. "Organic Charge Transfer Complexes"; Academic Press: New York, 1969.

(37) For a similar treatment of the Marcus equation in electron transfer, see ref 14.

acids.³⁸ Considering the crude model employed, we find it interesting that the estimate of the pK_a^A for HMB^+ lies near that obtained from the extrapolation of Figures 5a,b.³³ There is also chemical evidence which supports a value for the pK_a^A of HMB^+ near this range.

The trend in Table VIII reveals the acidities of the methylarene cation radicals to be a sensitive function of the number of methyl substituents. The same conclusion derives from Figure 5b in which the apparent Hammett ρ value is approximately -24 . We suggest that this rather sharp dropoff in acidity derives largely from the stabilization of the cation radical by methyl groups, which leads to extensive charge delocalization. Decreased solvation of such a highly delocalized cation in comparison to that of the pyridinium ion would account for the significant negative kinetic salt effect observed in the deprotonation rate constant k_2 (see Table IV).⁴⁰ A similar reasoning can also explain the relatively minor salt effects observed in the electron-transfer rate constant k_1 of hexamethylbenzene with the large, highly delocalized tris(phenanthroline)iron(III) oxidant.^{41,42}

Comments on the Mechanism for Proton Transfer from Methylarene Cation Radicals to Pyridine Bases. The Brønsted plot shown in Figure 4 for various methylarene cation radicals with different pyridine bases has a slope $\alpha = 0.26$. If this free energy relationship for proton transfer is considered in the context of the Marcus equation, the slope of such a magnitude corresponds to an overall free energy change ΔG° lying in the exergonic region of the driving force.⁴³ The kinetics results of the deuterium isotope effects in Table III lead to the same conclusion.⁴⁴ Thus the change in the deprotonation rate constant k_2 upon deuteration of the methylarenes derives directly from the experimental values of the rate constant ratio k_{-1}/k_2 . The kinetic isotope effect $k_2(\text{H})/k_2(\text{D})$ listed in Table VIII was obtained by simply dividing the values of $(k_{-1}/k_2)_\text{D}$ by those of $(k_{-1}/k_2)_\text{H}$, since the back electron transfer rate constant k_{-1} is the same for each isotopic methylarene (vide supra). The measure of the free energy change for the particular acid/base pair consisting of the methylarene and the substituted pyridine is given in Table VIII as $\Delta pK = (pK_a^A - pK_a^B)$. There is a clear trend in the Table for the deuterium kinetic isotope effect to decrease with an increasing driving force for proton transfer, consistent with an exergonic free energy change, which is provided by extrapolated values of pK_a^A estimated for the methylarene cation radicals.

We interpret thus the magnitude of the Brønsted slope and the trend in the kinetic isotope effect to reflect an early transition state in which proton transfer has not proceeded beyond the symmetrical situation.⁴⁶ Such a qualitative description of methylarene cation

radicals as acids accords with the relatively low sensitivity of proton-transfer rates to steric effects in the pyridine bases. Thus a pair of ortho-*tert*-butyl substituents are required to significantly perturb the Brønsted correlation of various pyridine bases in Figure 2.

Summary and Conclusions

The rates of oxidation of various methylarenes by the iron(III) complex $\text{Fe}(\text{phen})_3^{3+}$ in acetonitrile are regulated by the concentrations of added pyridine bases. This control allows the complete analysis of the kinetics for iron(III) disappearance according to the oxidation mechanism in Scheme II. Reliable values of the rate constant k_1 for the formation of methylarene cation radicals and the rate constant k_2 for their deprotonation can thus be evaluated for a variety of pyridine bases.

The rates of deprotonation of various methylarene cation radicals follow a general Brønsted relationship with the series of substituted pyridine bases included in Figure 4. This linear free energy correlation provides a quantitative measure of the relative acidities of methylarene cation radicals in the order hexamethylbenzene < pentamethylbenzene < durene \approx prehnitene (see ΔpK_a^A in Table VII). The acidity constant of hexamethylbenzene cation radical can be estimated on the basis of a long extrapolation of Figure 5a,b to toluene radical cation (for which the pK_a^A was recently evaluated by thermochemical analysis³³). The curvature in the Brønsted plot of the kinetic acidities is treated in the context of the Marcus equation, which provides a value for the intrinsic barrier to proton transfer in the range observed for other carbon acids. The magnitudes of the deuterium kinetic isotope effects and the kinetic salt effects can be interpreted in terms of a transition state in which proton transfer from the methylarene cation radical has only progressed partially. The limited hydrogen bonding to the base in the activated complex is indicated by the small steric effects of ortho-substituted pyridines. Such an early transition state is consistent with the Brønsted slope $\alpha = 0.26$, as interpreted by the Marcus formulation of proton transfer.

Experimental Section

Materials. The methylarenes hexamethylbenzene, pentamethylbenzene, and durene (Aldrich) were recrystallized from ethanol, followed by sublimation in vacuo. Prehnitene (Aldrich) was distilled in vacuo prior to use. Isodurene (Wiley Organics) was found to be 99.2% pure by analytical gas chromatography and used as such. Hexamethylbenzene-*d*₁₈ (Merck) was kindly donated to us by A. E. Nader (Du Pont). Durene-*d*₁₄ (KOR Isotopes) was used as purchased. Pyridine, 2,6-lutidine (Matheson, Coleman and Bell), 2,6-di-*tert*-butylpyridine, and 3-chloropyridine (Aldrich) were redistilled from KOH pellets before use. 4-Cyanopyridine (Aldrich) was recrystallized from ethanol. The other substituted pyridines used in this study were kindly donated to us by P. M. Zizelman.

Acetonitrile (HPLC grade from Fisher Scientific) was further purified by distillation from CaH_2 through a 15-plate Oldershaw column, followed by stirring overnight with KMnO_4 and Na_2CO_3 (5 g of each per liter). The mixture was filtered, distilled in vacuo, and finally fractionated from P_2O_5 under an argon atmosphere. The distillate was stored under argon in a Schlenk flask. Tetraethylammonium perchlorate (G. F. Smith Chemical Co.) was recrystallized from a mixture of ethanol and ethyl acetate. Tetra-*n*-butylammonium perchlorate (G. F. Smith) was recrystallized from a mixture of isooctane and ethyl acetate, followed by drying in vacuo in order to eliminate background reactions with the iron(III) complex. Lithium perchlorate (G. F. Smith) was dried in vacuo prior to use. The tris(phenanthroline)iron(III) complex $(\text{phen})_3\text{Fe}(\text{PF}_6)_3$ was prepared as described previously.¹⁴

Measurement of the Kinetics. The rate of disappearance of iron(III) was followed spectrophotometrically by measuring the concentration of FeL_3^{2+} at 510 nm ($\epsilon_{510} 1.10 \times 10^4 \text{ M}^{-1} \text{ cm}^{-1}$) with a UV-vis diode-array spectrometer (Hewlett-Packard Model 8450 A). At this monitoring wavelength the absorbance of the iron(III) complex was minor ($\epsilon_{510} 360 \text{ M}^{-1} \text{ cm}^{-1}$). All the kinetics studied were carried out in a 1.0-cm quartz cuvette which was flushed with argon. [The same results were obtained when extra precautions were taken to exclude air by using Schlenkware techniques.] The reactions were carried out in anhydrous acetonitrile solutions initially charged with ca. 0.1 mM FeL_3^{3+} and containing 0.1 M salt (LiClO_4 unless otherwise specified) and greater than 10-fold excess of the methylbenzene (3–100 mM) and the substi-

(38) (a) Kresge, A. *J. Chem. Soc. Rev.* **1973**, *2*, 475. (b) Kresge, A. *J. Acc. Chem. Res.* **1975**, *8*, 354.

(39) Dean, J. A. "Lange's Handbook of Chemistry", 12th ed.; McGraw-Hill: New York, 1979; pp 5–17 ff.

(40) (a) For a discussion of salt effects, see: Hammett, L. P. "Physical Organic Chemistry", 2nd ed.; McGraw-Hill: New York, 1970; Chapter 7. Amis, E. S. "Solvent Effects on Reaction Rates and Mechanisms"; Academic Press: New York, 1966. (b) For the effect of size on the solvation energies of methylarene cation radicals, see the discussion in ref 13.

(41) See: Brunshwig, B. S.; Creutz, C.; Macartney, D. H.; Sham, T.-K.; Sutin, N. *Faraday Discuss. Chem. Soc.* **1982**, *74*, 113.

(42) Note that the salt effects in methylarene oxidation by $\text{Fe}(\text{phen})_3^{3+}$ differs from that recently observed by Ebersohn⁵ for heteropoly tungstocobaltate anions. Since the latter are negatively charged, the electrostatic work terms for electron transfer are quite different.

(43) For a discussion of the Brønsted slopes in relation to the Marcus equation, see: (a) ref 27a, p 215 f. (b) Murdoch, J. R. *J. Am. Chem. Soc.* **1972**, *94*, 4410. (c) Murdoch, J. R.; Magnoli, D. E. *Ibid.* **1982**, *104*, 3792.

(44) For other examples of kinetic isotope effects in the deprotonation of methylarene cation radicals, see: (a) ref 5. (b) ref 18. (c) Parker, V. D. *Acta Chem. Scand., Ser. B* **1981**, *B35*, 123. (d) Sehestad, K.; Holcman, J. *J. Phys. Chem.* **1978**, *82*, 651. (e) Stewart, R. In "Isotopes in Organic Chemistry"; Buncl, E., Lee, C. C., Eds.; Elsevier: Amsterdam, 1976; Vol. 2, p 305 ff.

(45) Compare the discussion by Ebersohn⁵ and his tabulation of the kinetic isotope effects for the deprotonation of the cation radicals of various methylarenes.

(46) The maximum in the kinetic isotope effect has been observed in proton transfer from carbon acid when the driving force is zero. See p 250 ff of ref 27a (especially Figure 21) and Kresge, A. *J. Am. Chem. Soc.* **1980**, *102*, 7797.

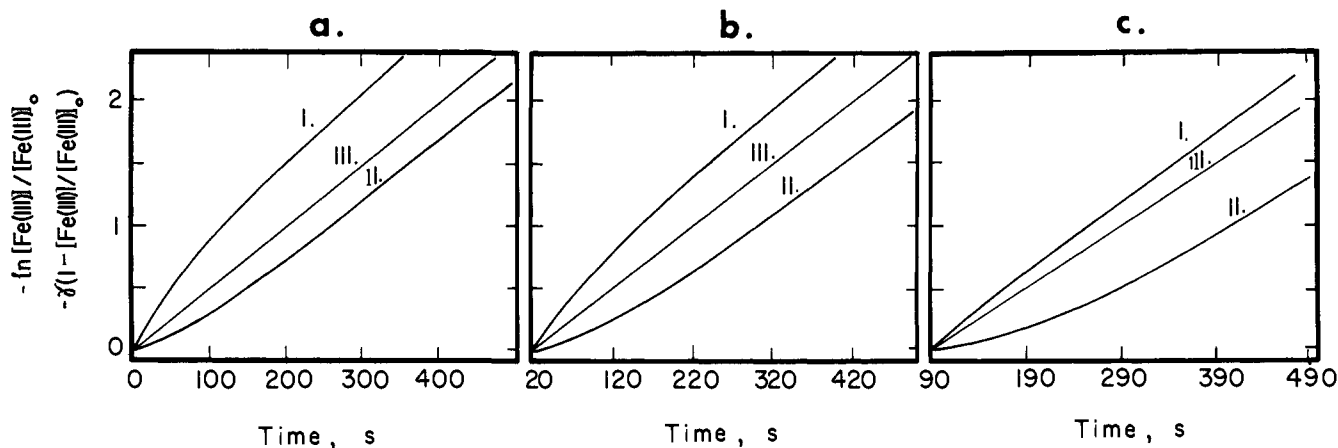


Figure 6. Rates of oxidative substitution of 40.5 mM pentamethylbenzene starting with 0.117 mM FeL_3^{3+} in acetonitrile containing 0.1 M LiClO_4 plotted as a function of $-\ln([\text{Fe(III)}]/[\text{Fe(III)}]_0) - \gamma(1 - [\text{Fe(II)}]/[\text{Fe(III)}]_0)$ according to eq 8 ($\gamma = 0$, curve I), eq 9 ($\gamma = 1$, curve II), and eq 12 ($0 < \gamma < 1$, curve III). The times at which the measurements were started are given in: (a) $t_{\text{exp}} \approx 0$ s, (b) $t_{\text{exp}} = 20$ s, and (c) $t_{\text{exp}} = 90$ s. Note the displacements of the scale along the abscissa.

tuted pyridines (9–500 mM) relative to the iron(III) oxidant. The rates of the competing background reactions were checked (for each methylbenzene and pyridine concentration employed) by first running controls which contained either the FeL_3^{3+} and arene only or the FeL_3^{3+} and base only. Generally, the background reaction for the least reactive arene constituted less than 25% over the time period required for 100% completion of the reaction of the relevant arene/base pair.

In a typical procedure, the quartz cell containing 1.8 mL of the saline solution of the methylbenzene and pyridine in excess was preequilibrated in the cell holder equipped with magnetic stirring (Hewlett-Packard Model 89101) and thermostated at 22 °C. Upon temperature equilibration, an aliquot (200 μL) of the iron(III) solution was quickly added to the solution with the aid of a hypodermic syringe, and the absorbance measurements began. The rates were usually followed to >99% conversion of iron(III). The absorbance A was related to the extent of reaction as $x = [\text{Fe(II)}]/[\text{Fe(III)}]_0 = (A_\infty - A_t)/(A_\infty - A_0)$ where A_∞ was the final absorbance obtained by averaging more than 10 absorbance measurements at the conclusion of the reaction, A_0 is the absorbance at the experimental time zero (i.e., $t_{\text{exp}} = 0$) and A_t is the absorbance at any time t .

The diode-array spectrometer was interfaced with a Digital Equipment Corp. 11/23 computer, and the absorbance data were transmitted directly for transformation to the form $\ln x = \ln([\text{Fe(II)}]/[\text{Fe(III)}]_0)$ and $(1 - x) = (1 - [\text{Fe(II)}]/[\text{Fe(III)}]_0)$ usable in the regression analysis. Values of $[\text{Fe(II)}]/[\text{Fe(III)}]_0$ were taken from 1.0 to 0.1 which correspond to 0–90% conversion, respectively. The multiple linear regression analysis using $\ln x$ and $(1 - x)$ as the independent variables and time as the dependent variable was accomplished by the MINC subroutine which was modified to accept 150 observations. The regression analysis was performed for each experiment at 3 values of x ranging from 1.0 to 0.5, 1.0 to 0.25, and 1.0 to 0.1, i.e., conversions of 50%, 75%, and 90%, respectively. This procedure ensured that uniform kinetics were obtained throughout each kinetics run. The validity of the procedure is shown in Table IX, in which the first, second, and third entries indicate the constancy of the measured values of the rate constant k_1 and the rate constant ratio k_{-1}/k_2 up to high conversions. Furthermore, the same reliability of the method is shown by the invariance of these rate constants with variations in the methylbenzene and pyridine concentrations.

Treatment of the Kinetics Data. The experimental determinations of the rate constant k_1 and the rate-constant ratio k_{-1}/k_2 according to eq 12 (and 13) are valid for the boundary condition that $[\text{Fe(II)}] = 0$ at $t = 0$. Such a condition can indeed be met experimentally in those kinetics runs which proceed at relative slow rates. However, we were interested in studying the kinetics behavior to high conversion (>90%) of $[\text{Fe(II)}]$, and we were forced to examine systems which were proceeding at faster rates than those allowed by the boundary conditions stated above. Under these restraints, we found that the measured values of k_1 and k_{-1}/k_2 were difficult to reproduce owing to inconsistency in precisely setting $t_0 = 0$; i.e., the mixing and start-up time could not be ignored.

Since the problem described above is a general one for any kinetics behavior which is a nonlinear function in the experimental variable (such as eq 9 and 12 for $[\text{Fe(II)}]/[\text{Fe(III)}]_0$ in our system), we will describe our corrective treatment in detail. We proceed by initially illustrating the problem graphically in Figure 6a–c in which the same rate is plotted as curve I = $-\ln([\text{Fe(II)}]/[\text{Fe(III)}]_0)$ according to eq 8, curve II = $-\ln([\text{Fe(II)}]/[\text{Fe(III)}]_0) + [\text{Fe(II)}]/[\text{Fe(III)}]_0 - 1$ according to eq 9, and

Table IX. Typical Results from the Effects of the Reaction Variables (Conversion and Initial Concentrations) on the Measured Rate Constants^a

ArCH ₃ , ^b mM	py, mM	conv, %	k_1 , M ⁻¹ s ⁻¹	k_{-1}/k_2 , 10 ⁻²
3.2	62	50	12	5.2
3.2	62	75	13	6.5
3.2	62	90	14	8.9
3.2	31	c	12	5.3
3.0	31	c	13	6.0
3.2	62	c	13	6.7
3.0	31	c	13	5.9

^a In acetonitrile solutions containing 0.1 mM FeL_3^{3+} and 0.1 M LiClO_4 at 22 °C. ^b Hexamethylbenzene. ^c Results averaged for conversions at 50%, 75%, and 90%.

curve III = $-\ln([\text{Fe(II)}]/[\text{Fe(III)}]_0) + \gamma(1 - [\text{Fe(II)}]/[\text{Fe(III)}]_0)$ according to eq 12. The plots in Figure 6a–c differ only by the time t_{exp} at which the initial data were taken, the scale on the abscissa being ~ 0 s in (a), 20 s in (b), and 90 s in (c), respectively. Thus depending on when the measurement is started after mixing, the rate given by curve III appears in Figure 6a to be closer to the limit defined by curve II. In contrast, the rate measurement for the same system, but commenced at a later time as indicated in Figure 6c, shows curve III to appear closer to the limit defined by curve I! Since this must clearly be an artifact arising from the nonlinear variation of a function of $[\text{Fe(II)}]/[\text{Fe(III)}]_0$, it underscores the importance of taking the starting time *explicitly* into account for the determination of the regression coefficients. This is most conveniently carried out by using the absorbance observed at the time defined as $t_{\text{exp}} = 0$ as a quantitative measure of the reduced iron(II) already produced in the system prior to the start of the kinetics measurement. Accordingly, the general rate law in eq 12 must be modified to

$$\ln \frac{[\text{Fe(II)}]}{[\text{Fe(III)}]_0} + G\gamma \left(1 - \frac{[\text{Fe(II)}]}{[\text{Fe(III)}]_0} \right) = \frac{-2k_1[\text{ArCH}_3]_0}{1+p} t_{\text{exp}} \quad (28)$$

where $G = (1 - A_0/A_\infty)/(1 - \epsilon_{\text{III}}/\epsilon_{\text{II}})$, as described in the derivation of the kinetics (vide infra). A_0 is the absorbance at $t_{\text{exp}} = 0$, A_∞ is the final absorbance, ϵ_{III} is the extinction coefficient of Fe(III) , and ϵ_{II} is the extinction coefficient of Fe(II) at the monitoring wavelength. Note that eq 28 is equivalent to eq 12 in its formulation except $\gamma = Gp/(1+p)$ rather than $\gamma = p/(1+p)$; and the values of γ evaluated by the regression analysis are accordingly $p = \gamma/(G-\gamma)$ rather than $p = \gamma/(1-\gamma)$. The correction by the G factor also applies to the limiting situation described by eq 9 which is modified to

$$\ln \frac{[\text{Fe(II)}]}{[\text{Fe(III)}]_0} + G \left(1 - \frac{[\text{Fe(II)}]}{[\text{Fe(III)}]_0} \right) = \frac{-2k_1[\text{ArCH}_3]_0}{p} t \quad (29)$$

In order to extract the relevant rate constants from the corrected rate law in eq 28, it was reparametrized in the form given in eq 13 by substitution of $k_a = 2k_1[\text{ArCH}_3]_0/(1+p)$, i.e.

$$-k_a^{-1} \ln \frac{[\text{Fe(II)}]}{[\text{Fe(III)}]_0} - G\gamma k_a^{-1} \left(1 - \frac{[\text{Fe(II)}]}{[\text{Fe(III)}]_0} \right) = t \quad (30)$$

Table X. Typical Correction for the Error in the Starting Time t_{exp} for the Kinetics Run Shown in Figure 6^a

t_{exp}^b (s)	γ^c	G^d	$\frac{\gamma^e}{1-\gamma}$	$\frac{\gamma^f}{G-\gamma}$
~0	0.66	0.89	1.94	2.86
20	0.52	0.70	1.08	2.86
50	0.38	0.53	0.61	2.53
90	0.29 ₅	0.40	0.42	2.86
120	0.26	0.34	0.35	3.25

^a The oxidation of 40.5 mM pentamethylbenzene by 0.117 mM total iron concentration in acetonitrile containing 250 mM 4-cyanopyridine. ^b experimental time at which the rate measurements actually commenced. ^c From the regression analysis according to eq 13. ^d $G = (1 - A_0/A_\infty)/(\epsilon_{\text{III}}/\epsilon_{\text{II}})$ from the absorbance measurement at t_{exp} . ^e Evaluated according to eq 12. ^f Evaluated according to eq 28.

[Note that eq 30 is equivalent to eq 13, except the formulation of eq 13 did not include the correction for t_{exp} . Multiple regression analysis (vide supra) was used to obtain the coefficients k_a and γ under conditions in which $\ln([Fe(II)]/[Fe(II)]_0)$ and $(1 - [Fe(II)]/[Fe(III)]_0)$ from the absorbance data corresponded to the independent, experimental variables. The validity of the correction is shown in Table X for the representative kinetics run illustrated in Figure 6. The regression coefficient listed in column 4 obtained from the uncorrected eq 13 is shown to be strongly dependent on t_{exp} , whereas the G correction according to eq 30 leads in column 5 to reliable values of γ even after relatively high conversions of iron(III).

The electron-transfer rate constant k_1 is obtained from the regression coefficients γ and k_a in eq 30 by the relationships: $k_1 = k_a(1+p)/2[ArCH_3]_0$ and $p = \gamma/(G-\gamma)$. Values of the rate-constant ratio k_{-1}/k_2 derive directly from eq 11.

Derivation of the Kinetics Rate Expression. The derivation of the kinetics was based on the stoichiometry in eq 4 and the mechanism prescribed in Scheme II under conditions in which the methylbenzene and pyridine were present in greater than 10-fold excess relative to the iron(III) oxidants. Since eq 7 is known to be fast,¹⁶ the rate of iron(III) disappearance is

$$-d[Fe(III)]/2dt = k_1[ArCH_3][Fe(III)] - k_{-1}[ArCH_3^+][Fe(II)] \quad (31)$$

Invoking the steady-state treatment for the transient intermediate $[ArCH_3^+]$ affords

$$-d[Fe(III)]/2dt = k_1[ArCH_3][Fe(III)](1 + k_{-1}[Fe(II)]/k_2[B])^{-1} \quad (32)$$

Since the experimental system is such that iron(II) may be present initially, let $C = [Fe(II)]_0 + [Fe(II)]_0$ at $t_{\text{exp}} = 0$. At any time t then, $[Fe(II)] = C - [Fe(III)]$. Substituting this quantity into eq 32 and separating the terms for integration yields

$$-\int_{[Fe(III)]_0}^{[Fe(III)]} \frac{d[Fe(III)]}{[Fe(III)]} - \frac{k_{-1}C}{k_2[B]} \int_{[Fe(III)]_0}^{[Fe(III)]} \frac{d[Fe(III)]}{[Fe(III)]} + \frac{k_{-1}}{k_2[B]} \int_{[Fe(III)]_0}^{[Fe(III)]} \frac{d[Fe(III)]}{[Fe(III)]} = 2k_1[ArCH_3]_0 \int_{t_{\text{exp}}=0}^t dt \quad (33)$$

Integration of eq 33, followed by simplification gives

$$\left[1 + \frac{k_{-1}C}{k_2[B]} \right] \ln \frac{[Fe(III)]}{[Fe(III)]_0} + \frac{k_{-1}[Fe(III)]_0}{k_2[B]} \left[1 - \frac{[Fe(III)]}{[Fe(III)]_0} \right] = -2k_1[ArCH_3]_0 t \quad (34)$$

In order to evaluate $[Fe(III)]_0$, we note that

$$[Fe(III)]_0 + [Fe(II)]_0 = C = A_\infty/\epsilon_{\text{II}} \quad (35)$$

when A_∞ is the final absorbance such that all the iron(III) has been reduced to iron(II), ϵ_{II} is the extinction coefficient of iron(II) at the monitoring wavelength. Since A_0 is the absorbance at $t_{\text{exp}} = 0$, it is given by

$$A_0 = [Fe(III)]_0\epsilon_{\text{III}} + [Fe(II)]_0\epsilon_{\text{II}} \quad (36)$$

The simultaneous solution of eq 35 and 36 yields

$$[Fe(III)]_0 = C(1 - A_0/A_\infty)/(1 - \epsilon_{\text{III}}/\epsilon_{\text{II}}) \quad (37)$$

Table XI. Relative Oxidation Potentials of Methylbenzene Cation Radicals Estimated by Several Independent Procedures^a

methylbenzene	relative oxidation potentials ΔE°			
	TFA ^b	E_p^c	Marcus ^d	Marcus ^e
hexamethylbenzene (HMB)	0.0	0.0	0.0	0.0
pentamethylbenzene (PMB)	0.13	0.02	0.13	0.13 ₃
durene (DUR)	0.21	0.24	0.16	0.20
prehnitene (PRE)	0.20	0.21	0.26	0.26

^a With hexamethylbenzene as the reference. ^b From E°_{Ar} in trifluoroacetic acid in ref 13. ^c From the correlation of E°_{Ar} in trifluoroacetic acid with E_p in acetonitrile from ref 13. ^d From the Marcus equation using the data in ref 14. ^e From the Marcus equation using the data in Tables I and II.

For convenience, let $x = [Fe(II)]/[Fe(II)]_0 = (A_\infty - A)/(A_\infty - A_0)$, $p = k_{-1}C/k_2[B]$, and $G = (1 - A_0/A_\infty)/(1 - \epsilon_{\text{III}}/\epsilon_{\text{II}})$. Substitution of these quantities into eq 34 leads to

$$(1+p) \ln x + pG(1-x) = -2k_1[ArCH_3]_0 t \quad (38)$$

which gives the form appropriate for regression analysis as

$$\frac{-1}{k_a} \ln x - \frac{\gamma'}{k_a}(1-x) = t \quad (39)$$

where $\gamma' = Gp/(1+p)$ and $k_a = 2k_1[ArCH_3]_0/(1+p)$.

Electrochemical Measurements. The electrochemical determination of the standard oxidation potential for the tris(phenanthroline)iron(II) complex was performed by cyclic voltammetry in acetonitrile containing 0.1 M TEAP. The CV wave was totally reversible ($i_p^c/i_p^a = 1.0$) for all the scan rates investigated (0.1–0.5 V s⁻¹). The working electrode consisted of a platinum disk of 1-mm diameter imbedded in a cobalt glass seal. It was polished with a 30- μ m silicon carbide abrasive and rinsed with water and acetone before use. The counterelectrode was a platinum mesh of ~ 1 cm² area. The reference electrode was a standard calomel electrode separated from the anolyte by a 0.1 M TEAP solution in acetonitrile. The potentiostat was a Princeton Applied Research Model 173 equipped with a Model 176 current/voltage converted for ohmic drop compensation and with a high impedance voltage amplifier (Model 178). The input potential was provided by a PAR Model 175 universal programmer, and the output was recorded on a Houston series 2000 x-y recorder. The standard reduction potential of $Fe(phen)_3(PF_6)_2$ was taken from the well-defined cathodic and anodic peak potentials as $E^\circ_{Ar} = (E_p^c + E_p^a)/2 = 1.09$ V vs. SCE.

The cyclic voltammograms of the methylbenzenes by and large showed irreversible chemical behavior at scan rate $\nu < 200$ V s⁻¹ in acetonitrile solutions. Irreversibility can be attributed to the short lifetimes of $ArCH_3^+$ caused by proton loss (compare eq 2 and 6) to solvent, since the cyclic voltammograms show reversible behavior in the more acidic trifluoroacetic acid medium. The relative oxidation potentials ΔE°_{Ar} of arene cation radicals in trifluoroacetic acid are listed in Table XI. There is a linear correlation between the standard oxidation potential E°_{Ar} obtained in trifluoroacetic acid and the anodic peak potentials E_p measured from the irreversible cyclic voltammograms in acetonitrile at a constant sweep rate.¹³ This relationship can be also used to estimate relative values of ΔE° for these methylarenes in acetonitrile, as listed in Table XI. The relative ΔE° for methylbenzene cation radicals can also be evaluated from the kinetics data ($\log k_1$) relating to the initial electron transfer step in eq 5. Thus the experimental free energy relationship between $\log k_1$ and the driving force $\mathcal{F}(E^\circ_{Fe} - E^\circ_{Ar})$ was fitted to the quadratic form of the Marcus outer-sphere equation using the measured values of the intrinsic barrier ($\Delta G^\circ_0 = 6.4$ kcal mol⁻¹). The relative values of ΔE° obtained from the data in ref 13 and that in Table I are also listed in Table XI. Although values of ΔE° estimated by these independent procedures are rather consistent, the standard deviations of ~ 0.03 V are too large to be of use in the measurement of $[pK_a^A]$ according to eq 25. Accordingly, we arbitrarily chose the values of ΔE° in the fifth column which were computed by the use of the Marcus equation, since our earlier studies demonstrated its applicability to the electron step in eq 5. An estimate of E°_{HMB} 1.50 V vs. SCE in acetonitrile was used for the computation of $\log k_2$ in Table V.¹⁴

Application of the Marcus Equation to Proton Transfer. The rate constant for the deprotonation of methylarene cation radicals in eq 19 can be reexpressed as

$$\Delta G^\circ = RT \ln(Z/k_2) = RT[\ln(Z/\kappa) + \mathcal{F}\Delta E/RT] \quad (40)$$

where $\Delta E = E^\circ_{Fe} - E^\circ_{Ar}$ and $Z = 10^{11}$. Since the work terms w_r and w_p are taken to be comparable in this acid-base system (see the text accompanying eq 27), the free energy change is

$$\Delta G^{\circ'} = 2.3RT[\text{p}K_a^A - \text{p}K_a^B] \quad (41)$$

The combination of eq 40 and 41 with the Marcus eq 26 yields

$$\log \kappa = A + B[\text{p}K_a^B] + C[\text{p}K_a^B]^2 \quad (42)$$

where $A = -(RT \ln 10)^{-1}\{w^r + \Delta G^{\circ}_0 + [\text{p}K_a^A](RT \ln 10)/2 + [\text{p}K_a^A]^2(RT \ln 10)^2/16\Delta G^{\circ}_0\} + \ln Z/n + \mathcal{F}\Delta E/RT$, $B = (RT \ln 10)^{-1} \cdot [\text{p}K_a^A]/8\Delta G^{\circ}_0 + 1/2$, and $C = -(RT \ln 10)/16\Delta G^{\circ}_0$. The solution of eq 42 was carried out by a polynomial regression analysis on a Digital Equipment Corp. 11/23 computer using a MINC basic subroutine in which $\log \kappa$ was the dependent variable and $[\text{p}K_a^B]$ the independent variable. The second-order coefficient $C = -0.013154$ yielded the values of ΔG°_0 , the first-order coefficient $B = 0.551694$ yielded the value of $[\text{p}K_a^A]$, and the zero-order term $A = -7.35117$ yielded the value of w^r with a correlation coefficient of 0.995 for all the data in Table V excluding 2,6-di-*tert*-butylpyridine (see text).

Acknowledgment. We thank J. Goncalves for the computer program for multiple regression analysis of the kinetics data, the National Science Foundation for financial support, and the United States-France (NSF-CNRS) cooperative program for the award of a fellowship to C.A.

Registry No. Fe(phen)₃(PF₆)₃, 28277-57-8; Dz, 7782-39-0; hexamethylbenzene, 87-85-4; pentamethylbenzene, 700-12-9; 1,2,4,5-tetramethylbenzene, 95-93-2; 1,2,3,4-tetramethylbenzene, 488-23-3; 1,2,3,5-tetramethylbenzene, 527-53-7; hexamethylbenzene cation radical, 34473-51-3; 1,2,4,5-tetramethylbenzene cation radical, 34473-49-9; pentamethylbenzene cation radical, 34473-50-2; 1,2,3,4-tetramethylbenzene cation radical, 34528-28-4; 2-fluoropyridine, 372-48-5; 2-chloropyridine, 109-09-1; 3-pyridinecarbonitrile, 100-54-9; 4-pyridinecarbonitrile, 100-48-1; 3-chloropyridine, 626-60-8; 3-fluoropyridine, 372-47-4; pyridine, 110-86-1.

Reaction Mechanisms of Oxidative Addition [H₂ + Pt⁰(PH₃)₂ → Pt^{II}(H)₂(PH₃)₂] and Reductive Elimination [Pt^{II}(H)(CH₃)(PH₃)₂ → CH₄ + Pt⁰(PH₃)₂]. Ab Initio MO Study

Shigeru Obara,^{1a,b} Kazuo Kitaura,^{1a,c} and Keiji Morokuma^{*1a}

Contribution from the Institute for Molecular Science, Myodaiji, Okazaki 444, Japan, and the Department of Chemistry, Kyoto University, Kyoto 606, Japan. Received March 5, 1984

Abstract: Reaction mechanisms of the oxidative addition of H₂ to two-coordinate Pt⁰(PH₃)₂ and the reductive elimination of CH₄ from four-coordinate Pt^{II}(H)(CH₃)(PH₃)₂ are studied by ab initio RHF and CI calculations with the energy gradient method within the framework of the relativistic effective core potential approximation for Pt core electrons. Fully optimized geometries of transition states of both reactions as well as the reactants and products have been obtained. The fact that the oxidative addition more commonly takes place for H₂ and only the reductive elimination does for CH₄ can be explained in terms of calculated exothermicity. The H₂ oxidative-addition reaction is suggested to pass through an early transition state that would lead directly to a *cis* product and then to be pushed toward a *trans* product by a steric repulsion between bulky phosphine ligands. A large deuterium kinetic isotope effect experimentally found in the reductive elimination reaction of CH₃D from Pt(D)(CH₃)(PPh₃)₂ is accounted for in terms of the calculated four-coordinate transition state, where the reaction coordinate is CPtH bending. A decrease in the interligand angle has been found to increase the reactivity of the metal center by selectively activating one of the d orbitals. Both donation and back-donation between the metal and H₂ have been found to be important at the transition state of the H₂ addition reaction.

The oxidative addition of molecular hydrogen and aliphatic RH and the corresponding reverse reductive elimination are important reactions as elementary processes in many catalytic and synthetic reactions.² Recent studies by Otsuka, Yoshida, and their colleagues on preparation and reaction of H₂ with two-coordinate platinum(0) [and palladium(0)] phosphine complexes present an interesting chemistry of homogeneous catalytic activities.³⁻⁵ Some of them easily absorb molecular hydrogen⁴ at room temperature to give dihydride complexes, which are identified by NMR and IR studies to be *trans* products. Oxidative-addition products have been found to be diamagnetic, indicating a closed-shell singlet ground state, which is reasonable for d⁸ square-planar complexes.⁶ Reversible reactions with H₂ at room temperature⁵ are also found for some of Pt(0)-chelating phosphine complexes. The symmetry

rule suggests that the oxidative addition of H₂ occurs in a *cis* fashion;² however, a *trans* mechanism has been proposed for the addition of H₂ to Ir complexes.⁷

The reductive-elimination reaction of CH₄ from Pt(H)-(CH₃)(PPh₃)₂ has been found by Abis, Sen, and Halpern.⁸ The reaction rate was unaffected by the presence of excess phosphine ligands, suggesting strongly that the elimination proceeds through a four-coordinate transition state. They observed a large deuterium kinetic isotope ratio of 3.3 for the decomposition reaction of Pt(D)(CH₃)(PPh₃)₂. On the other hand, small isotope ratios of 1.2-1.3 have been observed for H₂ and RH oxidative-addition reactions.^{9,10} The oxidative addition of aliphatic CH is considered to occur in a H-D exchange reaction of alkane with K₂PtCl₄¹¹ as a catalyst and in an internal metalation¹² where a CH bond in a ligand such as PR₃ is broken, although in both of the reactions the RH adduct has not been isolated. However, aromatic and olefinic CH's are known to add oxidatively to Ir, Pd, Fe, Ru, and Os compounds.¹³

(1) (a) Institute for Molecular Science. (b) Kyoto University. (c) Present address: Department of Chemistry, Osaka City University, Osaka 558, Japan.

(2) (a) Collman, J. P. *Acc. Chem. Res.* **1968**, *1*, 136. (b) Halpern, J. *Acc. Chem. Res.* **1970**, *3*, 386. (c) Vaska, L.; Werneke, M. F. *Trans. N. Y. Acad. Sci.* **1971**, *33*, 70. (d) Longato, B.; Morandini, F.; Bresadola, S. *Inorg. Chem.* **1976**, *15*, 650.

(3) Otsuka, S.; Yoshida, T.; Matsumoto, M.; Nakatsu, K. *J. Am. Chem. Soc.* **1976**, *98*, 5850.

(4) Yoshida, T.; Otsuka, S. *J. Am. Chem. Soc.* **1977**, *99*, 2134.

(5) Yoshida, T.; Yamagata, T.; Tulip, T. H.; Ibers, J. A.; Otsuka, S. *J. Am. Chem. Soc.* **1978**, *100*, 2063.

(6) Hartley, F. R. "The Chemistry of Platinum and Palladium"; Applied Science Publishers: London, 1973; Appendix II.

(7) Harrod, J. F.; Hamer, G.; Yorke, W. *J. Am. Chem. Soc.* **1979**, *101*, 3987.

(8) Abis, L.; Sen, A.; Halpern, J. *J. Am. Chem. Soc.* **1978**, *100*, 2915.

(9) Chock, P. B.; Halpern, J. *J. Am. Chem. Soc.* **1966**, *88*, 3511.

(10) Brown, J. M.; Parker, D. *Organometallics* **1982**, *1*, 950.

(11) Webster, D. E. *Adv. Organomet. Chem.* **1979**, *15*, 147.

(12) Goel, R. G.; Montemayor, R. G. *Inorg. Chem.* **1977**, *16*, 2183.